Mach-Zehnder interferometer polarization splitter in InGaAsP/InP

Document status and date:
Published: 01/01/1994

Document Version:
Publisher's PDF, also known as Version of Record (includes final page, issue and volume numbers)

Please check the document version of this publication:

• A submitted manuscript is the version of the article upon submission and before peer-review. There can be important differences between the submitted version and the official published version of record. People interested in the research are advised to contact the author for the final version of the publication, or visit the DOI to the publisher's website.
• The final author version and the galley proof are versions of the publication after peer review.
• The final published version features the final layout of the paper including the volume, issue and page numbers.

Link to publication

Mach-Zehnder Interferometer Polarization Splitter in InGaAsP/InP

L. B. Soldano, A. H. de Vreede, M. K. Smit, B. H. Verbeek, E. G. Metaal and F. H. Groen

Abstract—A passive TE/TM mode polarization splitter based on a Mach-Zehnder interferometer is demonstrated. Insertion loss of 1.5 dB and extinction ratios of −19 dB for TE and −15 dB for TM have been measured at 1510-nm wavelength. The device attains large optical bandwidth employing a pair of multimode interference (MMI) couplers and a wavelength-tolerant birefringent structure.

I. INTRODUCTION

SPATIAL TE/TM mode splitting is crucial for polarization diversity receivers [1], polarization shift keying [2] and polarization diversity multiplexing [3]. Several polarization splitters have been studied based on different operating principles. Asymmetric Y-branches on $LiNbO_3$ were reported [4] in which the effective indices were electro-optically controlled. The polarization-dependent phase shift in a pair of length-compensated nitride-loaded silicon-based waveguides was exploited in an interferometer polarization splitter [5]. Polarization splitters based on metal-cladded directional couplers in InGaAsP/InP were demonstrated [6]. More recently, a mode evolution splitter has been reported [7] which exploits the large birefringence of first-order modes in ridge waveguides. Here we report the design, fabrication and measurement results of a passive Mach-Zehnder Interferometer (MZI) polarization splitter in InGaAsP/InP. We demonstrate that waveguides with equal TE propagation constants — while still having a convenient difference in TM — can be realized by suitably loading a ridge waveguide with a dielectric (SiO_2) layer and a metal layer on top. Based on this concept, two *equal-length* waveguides (which we call differential arms) can be fabricated capable of providing the desired TM phase shift of π within the MZI, without introducing any TE phase shift. This approach has the advantage of avoiding the need of a critical compensating length in the differential arms, and/or the tuning of the waveguide widths.

II. PRINCIPLE OF OPERATION

A schematic layout of the Mach-Zehnder interferometer polarization splitter is shown in Fig. 1. The device consists

L. B. Soldano, A. H. de Vreede, M. K. Smit, and B. H. Verbeek are with Delft University of Technology, Faculty of Electrical Engineering, Laboratory of Telecommunication and Remote Sensing Technology, P.O. Box 5031, 2600 GA Delft, The Netherlands.

E. G. Metaal is with Royal PTT Nederland N.V., PTT Research Leidschendam, The Netherlands.

F. H. Groen is with Delft University of Technology, Faculty of Applied Physics, Research Group for Optics, The Netherlands.

IEEE Log Number 9400072.

of two 3-dB MMI couplers in restricted resonance [8], and a pair of non-equally birefringent straight waveguides of equal length (differential arms). These arms are designed in such a way as to present no relative phase shift for TE-polarization, and a relative phase shift of π for TM-polarization, i.e.

$$\Delta\varphi_{TE} = k_0\left(N_{TE}^{ms} - N_{TE}^{sl}\right)L_D = k_0\Delta N_{TE}L_D = 0 \quad (1)$$

$$\Delta\varphi_{TM} = k_0\left(N_{TM}^{ms} - N_{TM}^{sl}\right)L_D = k_0\Delta N_{TM}L_D = \pi \quad (2)$$

where $k_0 = 2\pi/\lambda$ is the wavenumber, λ is the free-space wavelength, N is the effective refractive index, L_D is the length of the differential arms, and the superscripts ms and sl refer to the metal-SiO_2 cladded waveguide and the strip-loaded waveguide respectively.

The first 3-dB coupler splits the (randomly polarized) input signal into two quadrature ($+90°$ relative phase) components, which are fed into the differential arms. Because of the equal TE propagation constants, the TE components will keep their relative phase ($+90°$) all along the differential arms and, when combined in the second 3-dB coupler, will add up and come out at the cross output port. The TM components, due to the phase shift of π introduced by one arm, will reach the second 3-dB coupler with a relative phase of $-90°$ and, when combined, will come out at the bar output port.

III. DESIGN CONSIDERATIONS

A metal layer applied directly on top of a ridge waveguide causes a very strong reduction in the TM effective index [6], with a small decrease in the TE effective index and a large attenuation for both polarizations. The inclusion of a (low-index) dielectric layer between the waveguide and the metal can compensate the TE index decrease and bring the propagation losses to acceptable levels [9], while still providing a useful difference in TM effective index. This allows the design of a metal-SiO_2 cladded waveguide with equal TE effective index as the strip-loaded waveguide. A cross section of the metal-SiO_2 cladded and strip-loaded waveguide structures is shown in Fig. 2.

The real and imaginary part of the effective indices were calculated for both structures by using the Effective Index Method with complex refractive indices for the metal layers [10]. The Fiedler and Schlachetzki model [11] was used to calculate the refractive index of InP and of lattice-matched quaternary $In_{0.72}Ga_{0.28}As_{0.61}P_{0.39}$ ($\lambda_g = 1.3 \ \mu m$) at different wavelengths. Fig. 3 shows the differences in the real part
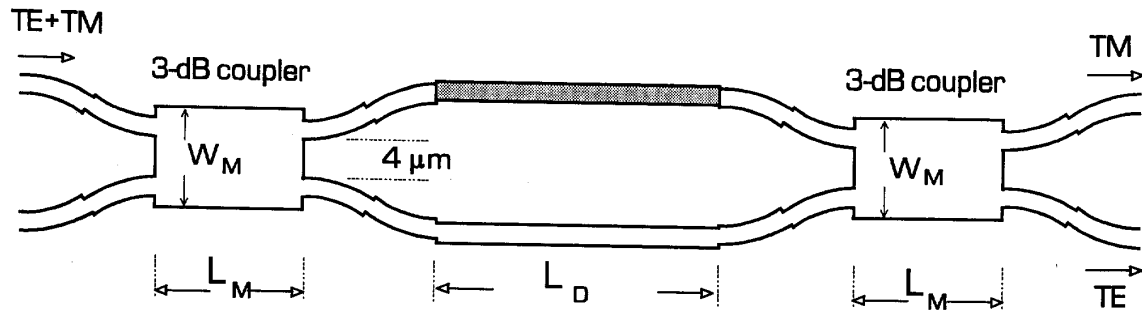
Fig. 1. Schematic layout of the Mach-Zehnder interferometer polarization splitter. It consists of two MMI 3-dB couplers with length L_M and width W_M, and a pair of differential arms of length L_D. The shaded area indicates the metal-SiO$_2$ cladding on top of the strip-loaded waveguide.
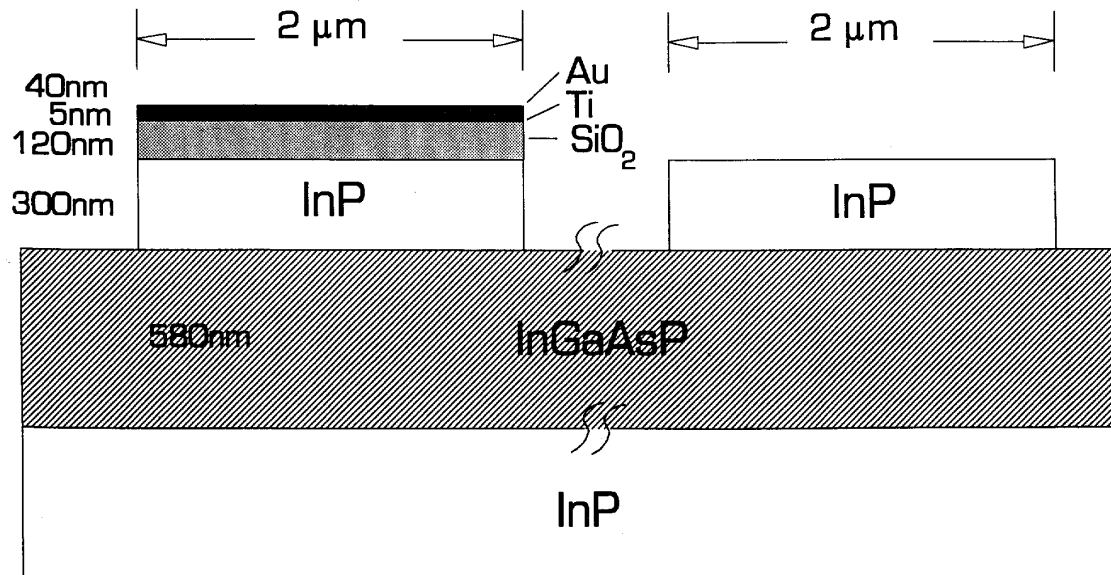

Fig. 2. Cross section of the metal-SiO$_2$ cladded waveguide (left) and the strip-loaded waveguide (right) structures. The refractive indices are: $n_{Au} = 0.18 - j10.2$, $n_{Ti} = 3.70 - j4.50$ [10], $n_{InP} = 3.17$, $n_{InGaAsP} = 3.39$ [11], and $n_{ox} = 1.444$ [17] at 1550-nm wavelength.

of the effective indices ΔN_{TE} and ΔN_{TM} (as defined in eqs. (1_ and (2)) between the metal-SiO$_2$ cladded and the strip-loaded waveguide, calculated as a function of the SiO$_2$ layer thickness d_{ox}. Metal layers thicker than 30 nm do not further modify the effective refractive index differences. At $d_{ox} \approx 120$ nm, we find $\Delta N_{TE} = 0$ which fulfills (1) for any value of L_D. For this value of d_{ox}, $\Delta N_{TM} = 4.3 \times 10^{-4}$ and (2) is thus fulfilled with $L_D = 1.76$ mm. The attenuation penalty due to the presence of metal in the metal-SiO$_2$ cladded waveguide decreases exponentially with the SiO$_2$ thickness, and for $d_{ox} = 120$ nm we calculated it to be ~1.8 dB/cm for TE and ~0.8 dB/cm for TM.

We used MMI couplers because of their good fabrication tolerances, polarization independence and large optical bandwidth [12]. All access waveguides were 2-μm wide. In order to minimize losses [13], lateral offsets were applied at the straight-to-curve transitions (0.15 μm) and at the curve-to-curve transitions (0.30 μm). The total device is 3.3-mm long,

which includes 1.0-mm radius curved access waveguides with a 50-μm separation.

IV. FABRICATION OF THE DEVICES

The devices were realized on a non-intentionally doped InP/InGaAsP/InP wafer grown by low-pressure MOVPE [14]. After sputtering a 120-nm SiO$_2$ film onto the whole wafer [17], a thin (~5 nm) Ti layer (to improve the adherence of Au) and a 40-nm Au layer were deposited by e-beam evaporation. The entire layout was first defined by a standard photolithography process and then patterned with two reactive-ion etching (RIE) steps. Metals and SiO$_2$ layers were etched in a CHF$_3$ plasma RIE. The 300-nm InP top layer was etched by a self-aligned CH$_4$:He RIE [15]. A second (non-critical alignment) standard photolithography covers one differential arm of the device, allowing the removal of the unwanted metals and SiO$_2$ by
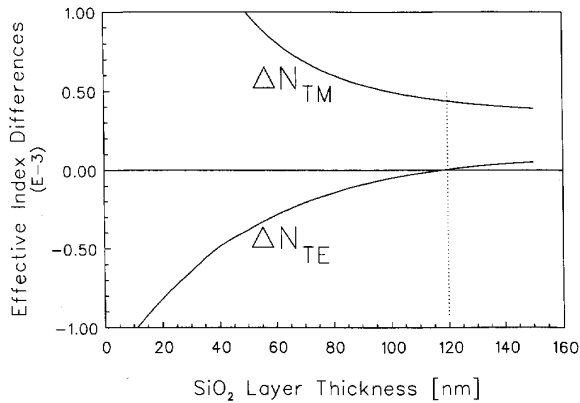
Fig. 3. Calculated refractive index differences ΔN_{TE} and ΔN_{TM} (from eqs. (1) and (2)) between the metal-SiO$_2$ cladded waveguide and the strip-loaded waveguide, as a function of SiO$_2$ layer thickness d_{ox}. The dotted line indicates the design value of d_{ox} for which $\Delta N_{TE} = 0$.

Fig. 4. Measured insertion loss and extinction ratio as a function of differential arms length L_D, obtained with a 1507-nm centre wavelength FP laser.

Fig. 5. Measured extinction ratio versus wavelength for a device with $L_D = 1.76$ mm obtained with an external cavity tunable laser. Each marker is the average of two measurements (one for each input), with the typical observed spread shown as vertical bars. Solid and dashed lines are parabolic fits.

wet chemical etching. The samples were anti-reflection coated by depositing a $\lambda/4$ layer of SiO$_x$ on the cleaved facets.

V. EXPERIMENTAL RESULTS

We fabricated a series of MZI polarization splitters with L_D varying from 1.5 to 2.0 mm in steps of 20 μm and MMI 3-dB couplers with $L_M = 425$ μm and $W_M = 15.8, 16.0$ and 16.2 μm. In order to test the individual performances of the MMI 3-dB couplers, we integrated a series of them with lengths L_M ranging from 415 to 435 μm in steps of 5 μm, and widths W_M ranging from 15.6 to 16.4 μm in steps of 0.2 μm. These 3-dB couplers showed excess loss below 1.0 dB and imbalance within ±0.5 dB, for a length tolerance of ±5 μm and a width tolerance of ±0.2 μm. Attenuation on 2-μm wide strip-loaded straight (reference) waveguides was determined to be 1.2 dB/cm for TE and 2.8 dB/cm for TM, from transmission measurements, a two-dimensional overlap calculation of the mode mismatch, and an analytical approximation of the facet reflectivity [16]. These results agree to within ±0.3 dB/cm with loss measurements performed on similar waveguide structures by the Fabry-Perot resonance method. The metal-SiO$_2$ cladded waveguides showed attenuations of 3.3 dB/cm for TE and 3.7 dB/cm for TM.

The MZI polarization splitters were characterized by launching alternatively TE- and TM-polarized light into one input, recording the light from both outputs and repeating the process for the other input. Light was end-fire coupled by focusing a pair of 40× IR anti-reflection coated microscope objectives at the cleaved facets. The outputs were imaged onto a Ge photodiode and read by a lock-in amplifier.

Fig. 4 shows the insertion loss and extinction ratio measured with a 1507-nm Fabry-Perot laser on a number of devices with varying L_D. Typical insertion loss of 1.5 dB (with respect to straight reference waveguides) was observed for both polarizations in the vicinity of $L_D = 1.76$ mm. As expected, TE extinction ratio remains quite constant for all devices. Its slight droop is most probably due to the fact that
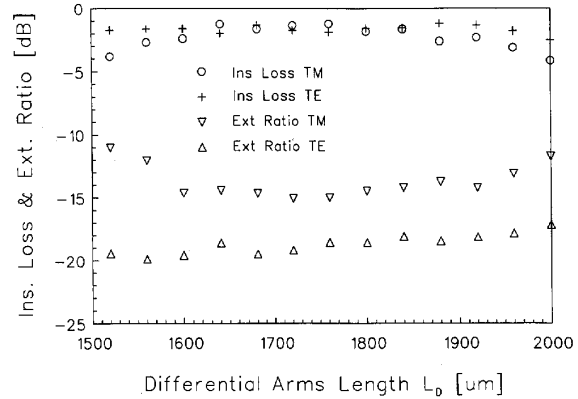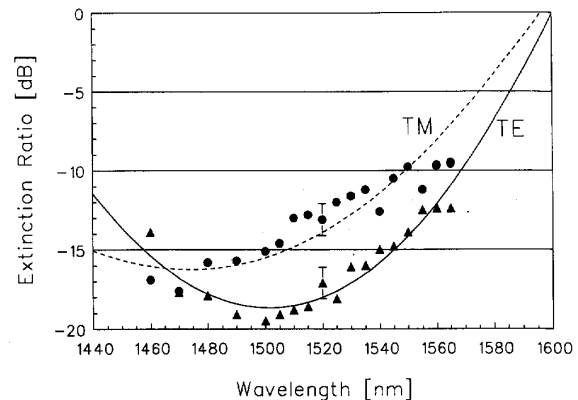
ΔN_{TE} (though very low) is not exactly zero. The extinction ratio for TM shows a soft maximum around $L_D = 1.76$ mm. The difference between TE and TM extinction ratios is partly due to a somewhat larger TM imbalance in the MMI 3-dB couplers.

Fig. 5 shows the extinction ratio as a function of the wavelength, measured on a device with design value dimensions ($L_D = 1.76$ mm, $L_M = 425$ μm and $W_M = 16.0$ μm). Each marker represents the average of two measurements (one for each excited input port). The best TE extinction ratio was -19 dB at 1500 nm, in good agreement with the design wavelength of 1510 nm. TM reaches a best extinction ratio of -17 dB at 1470 nm. We attribute this discrepancy to the uncertainty in the value of the metals refractive indices. Over a 60-nm wavelength range the TE (TM) extinction ratio remains below -16 dB (-13 dB).

VI. CONCLUSION

A polarization splitter based on a Mach-Zehnder interferometer has been demonstrated. The desired TE and TM

phase shifts were realized with a metal-SiO_2 cladding on a strip-loaded waveguide. The devices were fabricated in In-GaAsP/InP waveguides with a rather simple two-mask process. The design requires, however, a good control of the SiO_2 layer thickness and its refractive index, in order to accurately compensate the influence of the metal layer for TE polarization. For example, a ±10% deviation from the optimum SiO_2 layer thickness would result in a 5-dB penalty in the extinction ratio. At 1510-nm, we measured extinction ratios of −19 dB for TE and −15 dB for TM, insertion losses of about 1.5 dB for both polarizations, and large bandwidth.

ACKNOWLEDGMENT

REFERENCES

[1] T. Okoshi, S. Ryn and K. Kikuchi, "Polarization diversity receiver for heterodyne/coherent optical fiber communications," in *Proc. IOOC/OFC'83*, Tokyo, Japan, 1983, paper 30C3-2.

[2] K. Fukuchi, S. Yamazaki, T. Ono and M. Rangaraj, "Polarization shift keying—direct detection scheme for fiber nonlinear effect insensitive communication system," in *Proc. European Conference on Optical Communication ECOC'92*, Berlin, Germany, 1992, pp. 169–172.

[3] F. Heismann, P. B. Hansen, S. K. Korotky, G. Raybon, J. J. Veselka and M. S. Whalen, "Automatic polarization demultiplexer for polarization-multiplexed transmission systems," in *Proc. European Conference on Optical Communication ECOC'93*, Montreux, Switzerland, 1993, pp. 401–404.

[4] M. Masuda and G. L. Yip, "An optical TE-TM mode splitter using a LiNbO₃ branching waveguide," *Appl. Phys. Lett.*, vol. 37, pp. 20–22, 1980.

[5] Y. Shani, C. H. Henry, R. C. Kistler and K. J. Orlowsky, "Four-port integrated optic polarization splitter," *Appl. Opt.*, vol. 29, no. 3, pp. 337–339, 1990.

[6] P. Albrecht, M. Hamacher, H. Heidrich, D. Hoffmann, H.-P. Nolting and C. M. Weinert, "TE/TM mode splitters on InGaAsP/InP," *IEEE Photon. Technol. Lett.*, vol. 2, no. 2, pp. 114–115, 1990.

[7] J. W. Pedersen, J. J. G. M. van der Tol, E. G. Metaal, Y. S. Oei, F. H. Groen and I. Moerman, "Realization of a mode evolution polarization splitter on InGaAsP/InP," in *Proc. European Conference on Optical Communications ECOC'93*, Montreux, Switzerland, 1993, post-deadline paper ThC12.3.

[8] L. B. Soldano, F. B. Veerman, M. K. Smit, B. H. Verbeek, A. H. Dubost and E. C. M. Pennings, "Planar monomode optical couplers based on multimode interference effects," *J. Lightwave Technol.*, vol. 10, no. 12, pp. 1843–1850, 1992.

[9] S. C. Rashleigh, "Four-layer metal-clad thin film optical waveguides," *Optical and Quantum Electronics*, vol. 8, pp. 49–60, 1976.

[10] M. A. Ordal, L. L. Long, R. J. Bell, S. E. Bell, R. R. Bell, R. W. Alexander and C. A. Ward, "Optical properties of the metals Al, Co, Cu, Au, Fe, Pb, Ni, Pd, Pt, Ag, Ti, and W in the infrared and near infrared," *Appl. Opt.*, vol. 22, no. 7, pp. 1099–1119, 1983.

[11] F. Fiedler and A. Schlachetzki, "Optical parameters of InP-based waveguides," *Solid-State Electron.*, vol. 30, no. 1, pp. 73–83, 1987.

[12] L. B. Soldano, M. Bachmann, P.-A. Besse, M. K. Smit and H. Melchior, "Large optical bandwidth of InGaAsP/InP multi-mode interference 3-dB couplers," in *Proc. European Conference on Integrated Optics ECIO'93*, Neuchâtel, Switzerland, 1993, paper 14-10.

[13] E. C. M. Pennings, Bends in Optical Ridge Waveguides, Modeling and Experiments, *Ph.D. Thesis*, Delft University of Technology, 1990. ISBN 90-9003413-7.

[14] I. Moerman, G. Coudenys, P. Demeester, B. Turner and J. Cawley, "Influence of gas mixing on the lateral uniformity in horizontal MOVPE reactors," *J. Cryst. Growth*, vol. 107, pp. 175–180, 1991.

[15] L. H. Spiekman, F. P. G. M. van Ham, M. Kroonwijk, Y. S. Oei, J. J. G. M. van der Tol, F. H. Groen and G. Coudenys, "A new fabrication process for very low-loss narrow-width InGaAsP/InP waveguides," in *Proc. European Conference on Integrated Optics ECIO'93*, Neuchâtel, Switzerland, 1993, paper 2-30.

[16] J. Buus, "Analytical approximation for the reflectivity of DH lasers," *IEEE J. Quantum Electron.*, vol. QE-17, no. 12, pp. 2256–2257, 1981.

[17] M. K. Smit, "Integrated Optis in Silicon-based Aluminum Oxide", *Ph.D. Thesis*, Delft University of Technology, 1991. ISBN 90-9004261-X.